Arch. Min. Sci. **70** (2025), 3, 359-376

Electronic version (in color) of this paper is available: http://mining.archives.pl

DOI: https://doi.org/10.24425/ams.2025.156289

KATARZYNA CYRAN[1], MICHAŁ KOWALSKI[1*]

INFLUENCE OF GEOTECHNICAL FACTORS ON SLOPE STABILITY IN THE WESTERN BIELAWY LIMESTONE OPEN-PIT MINE (POLAND)

The stability of the slope is closely related to the safety of mining operations, rational excavation planning, and the optimal utilization of the deposit. The stability of an open-pit mine is controlled by both geotechnical and geological factors. Thus, this study aimed to investigate the influence of complex geological conditions like karst, tectonics, and lithology on the stability of the northern slope of the Western Bielawy limestone open-pit mine in central Poland. The site, located within the Barcin-Piechcin-Pakość limestone deposit, exhibits complex lithological variability, karst features, and tectonic disturbances. An integrated approach, combining laboratory testing, detailed rock mass characterization, and numerical modelling, was employed to assess slope stability. A 3D numerical model of the northern slope was used to evaluate stability under the planned excavation geometry. Numerical simulations, conducted with FLAC3D software, employed the Modified Shear Strength Reduction Method. The results showed that the initially planned slope geometry yielded a safety factor below acceptable thresholds due to weak, fractured claystones and weathered limestones. By modifying bench widths and reducing the slope angle, the safety factor was improved to meet the minimum required value of 1.30. The study demonstrates the necessity of integrating geological, geotechnical, and numerical methods for reliable slope stability assessments. These findings provide valuable insights for optimizing excavation designs in carbonate formations affected by tectonic and weathering processes.

Keywords: Slope stability; complex geotechnical conditions; numerical analysis; slope angle; bench width

1. Introduction

The rock slope stability is a principal concern in open-pit mines due to its impact on mining operations' safety. Therefore, this issue is continuously studied by researchers and engineers and

[1] AGH UNIVERSITY OF KRAKOW, FACULTY OF CIVIL ENGINEERING AND RESOURCE MANAGEMENT, AL. ADAMA MICKIEWICZA 30, 30-059 KRAKOW, POLAND

* Correspondence author: kowalski@agh.edu.pl

approached using various methods. Furthermore, in large scale open-pit mines, the slope angle gradually increases, becoming steeper, which affects both mining operations costs and safety requirements [1,2].

The slope failures are typically caused by the interaction of geological, geomorphological, and climate factors. Consequently, accurately determining the physical and mechanical properties of rock mass is a critical part of stability analysis [1-4].

The stability of slopes in open-pit mines is commonly analysed using numerical simulations. This method has proven to be highly effective and has become increasingly popular [5]. Stability conditions in limestone open-pit mines have been described in several studies [6-9]. Numerical analysis considering the role of geological factors in slope stability have been investigated by Yang et al. [5], Saadoun et al. [4], Zhang et al. [3] including weathering factors [1,10,11]. Onyango et al. [12] applied numerical modelling to evaluate slope stability in a coastal limestone quarry, while Liu et al. [13] conducted numerical simulations using FLAC3D combined with limit equilibrium methods to investigate instability and slope failure mechanisms in a limestone quarry in Weibei, China. This paper primarily addresses slope stability problems through numerical modelling simulations, focusing on complex geological conditions.

The Western Bielawy open-pit mine, located in central Poland is the largest limestone quarry in Central Poland. With over a century of continuous operation, the site has faced numerous challenges related to slope stability, driven by geological and geomorphological factors as well as rainfall. These factors create complex geotechnical conditions that must be carefully considered in the design and operation of open-pit excavations.

The objective of this study is to evaluate the influence of geological conditions, such as local karst processes, tectonic disturbances, and variable lithology, on the stability of the northern slope at the Western Bielawy open-pit mine. The paper presents an integrated approach combining laboratory testing, detailed rock mass characterization, and numerical modelling to simulate different slope geometries. This approach aims to determine optimal excavation configurations and the best utilization strategies for the limestone deposit.

The methodology presented in this paper can be applied in the development of open-pit mines and the planning of exploitation in limestones deposits disturbed by tectonics, as well as those characterised by a variety of petrological features and variations in mechanical parameters.

2. Engineering geology of the Western Bielawy open pit mine

2.1. Geological data

The Western Bielawy open-pit mine is located in Kujawy region. It is part of the Barcin-Piechcin-Pakość limestones deposit, which is excavated in 4 open-pit mines: Western Bielawy, Eastern Bielawy, Western Wapienno and Eastern Wapienno. The Upper Jurassic limestones and marlstones (Fig. 1) excavated by the open-pit mine are part of SW limb of the Zalesie anticline (Fig. 2), situated at the border of the Kujavian segment of the Polish Trough [14-16]. The Zalesie anticline formed due to the holokinetic uplifting of the Upper Permian (Zechstein) rock salts from the substrate, consisting of Mesozoic sediments (Fig. 2). The Upper Jurassic limestones and marlstone are overlain by Pleistocene formations (overburden) mainly moraine clays, sands, and gravels, ranging from 3 to over 30 m in thickness [17,18]. The lithostratigraphic profile of Upper Jurassic strata (Fig. 1) is divided into several units [19]. The A unit consists mainly dark marly

claystones and marlstone, with thicknesses ranging from 5 m in the centre of Zalesie anticline to 200 m thick in the limbs. The B and C units (Fig. 1) are represented by various kinds of organic limestones and marlstone which are further subdivided into [19]:

- B1 – clays, marlstones, and marly limestones (thickness from several to 30 m),
- B2 – massive limestones (thickness from 120 m to 220 m),
- B3/B4 – limestones with *foraminifera*, marly limestones, locally marlstones (thickness from several to 140 m),
- B5 – massive limestones, marlstones (thickness about 40 m),
- C1/C2/C3 – micritic limestones, marly limestones and marlstone (thickness about 100 m).

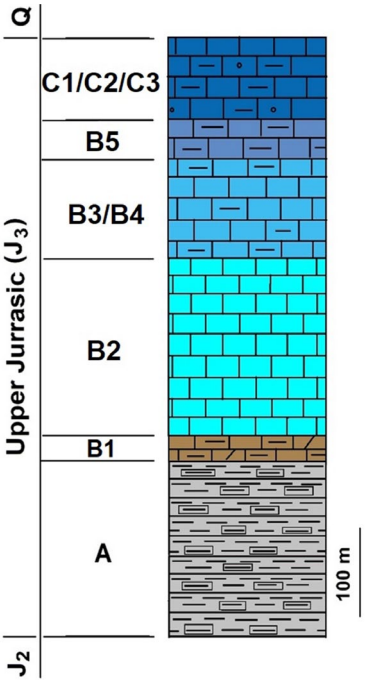

Fig. 1. Schematic lithostratigraphic profile of Upper Jurassic strata (based on [19])

The massive limestones of B2 are primarily excavated, as well as limestones of B3/B4. Middle and Lower Jurassic sandstones, claystones, siltstones, and dolomites underlie the Upper Jurassic strata [14].

The tectonics of the area is determined by longitudinal dislocations in NW-SE directions and lateral slip faults associated with Zalesie anticline (Fig. 2). The limestones and marlstone strata are located in SW limb of this anticline, characterised by dip of 12-22° towards SW. There are two main fault systems: lateral NE-SW or NNE-SSW which dominates, and longitudinal NW-SE [14]. Moreover, the limestones are affected by numerous karst phenomena like channels, packets, and cavities.

Open-pit mining at Western Bielawy has been carried out on two (northern and southern) pit wall slopes and 4 mining benches with an elevations of +28 m a.s.l., +40 m a.s.l., +60 m a.s.l. and +80 m a.s.l. Next 3 mining benches, at elevations of –6 m a.s.l., –20 m a.s.l., +14 m a.s.l. were formed starting from 2018, along with the steepening of the entire pit wall (Fig. 3). The Upper Jurassic beds that form the northern slope of the Western Bielawy open-pit are the most differentiated in terms of petrology and the intensity of karstic weathering. The border between the Quaternary overburden and the Upper Jurassic beds was determined at elevations ranging from +52.46 to +102.80 m a.s.l., while the boundary between the Upper Jurassic beds and Middle Jurassic beds is located between –16.65 to +50.31 m a.s.l.

2.2. Lithological characteristic of rock formations

The characteristics of the sediments in the Western Bielawy open-pit mine were determined based on cores obtained from eight boreholes drilled in 2018. The drilling was conducted to

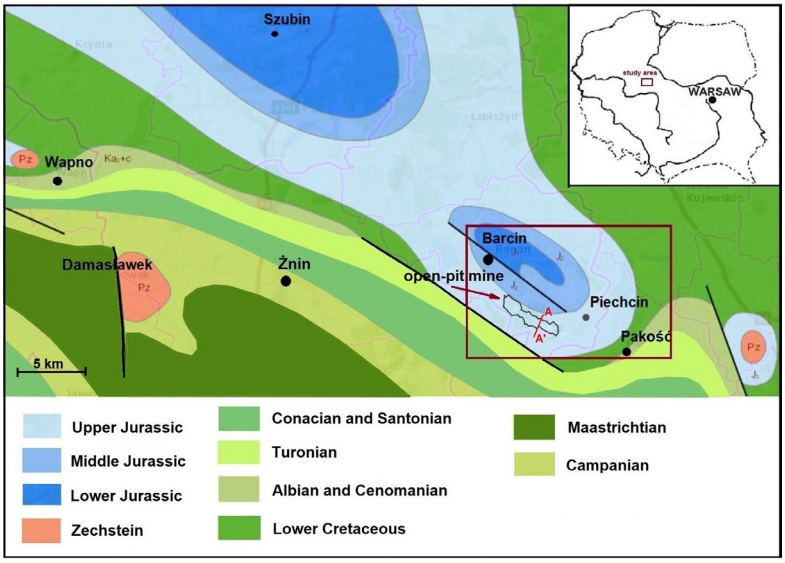

Fig. 2. Geological map of the area of Barcin-Piechcin-Pakość deposit [20]

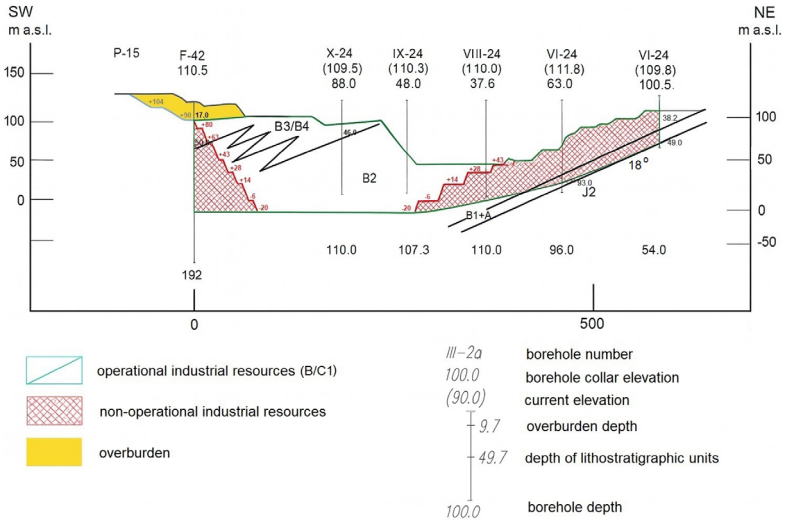

Fig. 3. Geological cross-section through Western Bielawy open-pit mine [21 modified]

identify the boundary between the Upper and Middle Jurassic sediments and to recognize the detailed lithology of the sediments. The sediments displayed in the drilling cores are lithologically differentiated (Fig. 4), ranging from limestones and marly limestones to marlstone and claystones.

In the analyzed cores, most of the sediments were affected by tectonic processes (Fig. 5). Limestones, marly limestones, and marlstones exhibit systems of irregular fractures. Claystones were severely fractured, slickensided, and fragmented into cubes. At the boundary between the

Age/Unit	Borehole	Depth [m]	Lithology	Description	Photo
J_3/ C1/C2/C3	GT-12.1	84.4-84.8 85.4-85.8	marly limestone/ marlstone	Grey/white partially laminated marly limestone passing in laminated marlstone, laminae are irregular wavy, load deformations like load casts and pseudonodules are visible	
J_3/ B3/B4	GT-5.2	57.3-57.7 58.3-58.7	marly limestone/ marlstone	Grey/white laminated marlstone passing in marly limestone, laminae are irregular wavy, load deformations like load casts and pseudonodules are visible	
J_3/ B2	GT-5	23.6-24.0 24.6-25.0	weathered limestone (karst)	Grey, fractured limestone with irregular cavities filled with calcite crystals 2.0-3.0 cm in diameter and single bigger cavity above 10 cm in diameter	

J_3/ B2	GT-5.2	31.0-31.4 32.0-32.4	weathered limestone (karst)	Grey, fractured limestone, irregular calcite veins cut limestone in different directions, single cavities 0.5-1.5 cm in diameter are visible,	
	GT-6	8.0-8.4 .9.0-9.4	limestone with debris	White fractured limestone partially severely weathered with debris	
	GT-6	42.5-42.9 43.5-43.9	massive limestone	White laminated limestone, load deformations like load casts and pseudonodules are visible	

J_3/ B1+A	GT-12.1	85.6-86.0 86.6-87.0	marlstone	Dark grey/black laminated marlstone, laminae are irregular wavy, load deformations like load casts, pseudonodules and flame structures are visible	
	GT-5.2	60.3-60.7 61.3-61.7	marly limestone	Grey laminated marly limestone, laminae are irregular wavy, load deformations like load casts and pseudonodules are visible	
J_2	GT-5.1	56.0-56.4 57.0-57.4	claystone	Dark brow/black fractured and laminated claystone	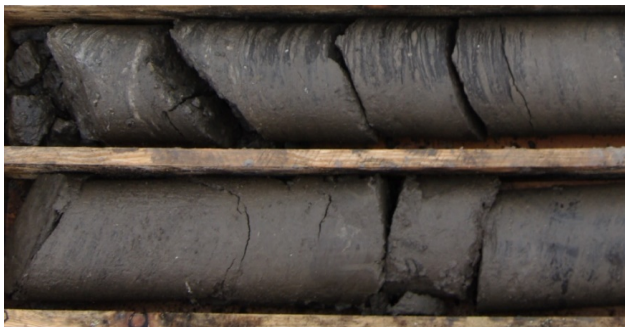

Fig. 4. Lithology of sediments in the Western Bielawy

Upper and Middle Jurassic sediments, brecciated limestones, marlstones, and claystones were found. Marlstones and claystones were severely slickensided and divided into slices. Moreover, the limestones show evidence of severe chemical weathering (karstification), such as voids (1-10 cm), voids filled with calcite crystals, and calcite veins (1-2 cm thick), which likely represent fracture fillings. Irregular or wavy laminae, load deformations such as load casts, pseudonodules, and flame structures are visible in the marlstones and marly limestones. These structures result from the loading of unconsolidated sediments. Additionally, a gradual transition from limestone through marl to claystone occurs over a short distance (40-60 cm) in many cores.

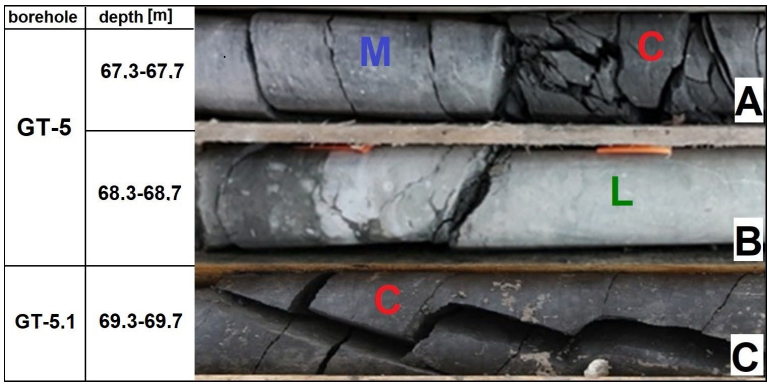

Fig. 5. Indicators of tectonic processes visible in drilling cores of claystones (C), marlstones (M) and marly limestones (L): A: fracturing and fragmentation, B: brecciation, C: fracturing

2.3. Geotechnical properties

Based on the petrological description of cores, as well as geological and stratigraphical data, five geotechnical layers were distinguished within the Jurassic sediments from the northern slope of the Western Bielawy pit-mine:

- marly limestone and marlstone (J_3 C1/C2/C3),
- marly limestone and marlstone (J_3 B3/B4),
- weathered limestone and massive limestone (J_3 B2),
- marly limestone and marlstone (J_3 A+B1),
- claystone (J_2).

The estimation of the rock mass properties was based on the Hoek and Brown failure criterion [22,23] which employs the Geological Strength Index (GSI), uniaxial compressive strength, and the Hoek-Brown constant m_i. Moreover, to improve the description of the rock mass quality, the Rock Quality Designation (RQD) was determined.

The GSI system is based on the assessment of the following factors: lithology, structure and condition of discontinuities surfaces in the rock mass [24]. The GSI is estimated through visual examination of the rock mass encountered in tunnels, slopes, and drilling cores [25].

The RQD [26] is used to asses rock quality and degree of jointing, fracturing, and shearing in the rock mass [16]. It is defined as the ratio of intact drill core pieces larger than 10 cm and total core length.

Additional verification of the mentioned factors was carried out by determining the GSI values expressed as an equation [27], involving the joints condition $JCond_{89}$ value defined by Bieniawski [28] and RQD value:

$$GSI = 1.5 \times JCond^{89} + RQD/2$$

Samples for the mechanical tests were selected from cores (drilled in 2018) and represented each geotechnical layer and lithological type. Uniaxial compressive strength (UCS) tests were conducted on limestones, marlstone, and marly limestones. Most claystones were severely fractured and slickensided, which resulted in the defragmentation of the cores. Claystone samples for direct shear tests were selected from the fractured core parts. However, those parts of the cores in which claystone was suitable for making cylindrical samples were tested for uniaxial compressive strength. The mechanical parameters obtained in the laboratory tests are listed in the table (TABLE 1). The friction angle and cohesion of marlstones and limestones were calculated using RockLab software.

The mechanical properties of Upper and Middle Jurassic rocks for each geotechnical layer were calculated as the weighted average, considering the percentage contribution of each lithological type's thickness and the values of the corresponding parameters determined in the laboratory tests (Fig. 6). The high lithological diversity of sediments within one geotechnical layer caused the values of these parameters to vary widely. For example, the average GSI for B2(J_3) is 55, but the estimated values range from 46 to 65 (Fig. 6). Moreover, geotechnical parameters are differentiated within each lithological type. Thus, the average value and the range for each parameter are presented in a table (TABLE 2).

TABLE 1

Average geotechnical parameters for geotechnical layers

Strata/age	Structure	Joints quality	GSI	RQD [%]	$JCond_{89}$	m_i	*Rc* [MPa]	ρ [g/cm^3]	*c* [MPa]	φ [^{o}]
C1/C2/C3 (J_3)	BB	fair	46	52	13	10	14.16	2.59	0.171	28.94
B3/B4 (J_3)	BB	good/fair	50	57	15	11	19.95	2.61	0.236	34.74
B2 (J_3)	B	fair	55	74	16	11	44.29	2.72	0.404	43.09
B1+A (J_3)	BB	fair/poor	40	48	12	8	15.60	2.51	0.142	25.44
(J_2)	BNP	poor	28	26	9	4	6.10	2.17	0.069	15.28

TABLE 2

Geotechnical parameters for lithological type

Lithology	Number of samples	*Rc* [MPa] range	Average *Rc* [MPa]	ρ [g/cm^3] range	Average ρ [g/cm^3]
marly limestone	6	16.03-26.37	19.69	2.29-2.50	2.61
marlstone	7	10.04-16.74	12.55	2.14-2.47	2.48
weathered limestone (karst) with cavities	7	51.23-35.80	43.75	2.58-2.72	2.65
weathered limestone (karst) with calcite veins	6	24.97-42.43	33.72	2.68-2.74	2.70
massive limestone	8	70.22-72.11	72.35	2.90-2.95	2.90
claystone	6	3.38-6.46	4.76	2.08-2.25	2.16

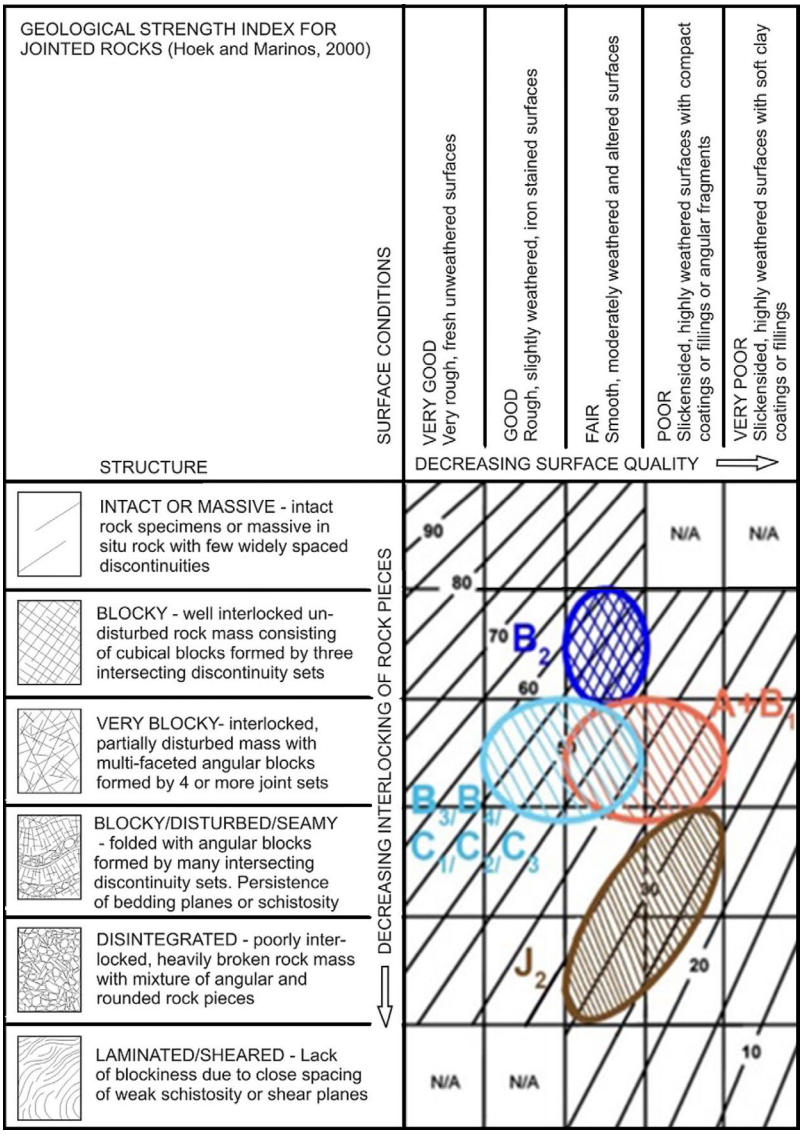

Fig. 6. GSI values for geotechnical layers

3. Methodology of numerical simulations

The geological structure of the northern slope of the Western Bielawy open-pit was projected in 3D numerical model based on geological cross-sections, prepared for the deposit documentation. The cross-sections reflect information obtained from boreholes drilled since the 1960s. Additionally, borehole data from drilling conducted in 2017 and 2018 [29] were taken into account in building the numerical model.

Based on the described geotechnical data, the following layers were distinguished in the numerical model:

- Quaternary clays and silty clays (Q, overburden),
- Quaternary sands, gravels, and sandy clays (Q, overburden),
- Upper Jurassic limestones and marly limestones (J_3 B3/B4),
- Upper Jurassic micritic limestones, marlstones, and marly limestones (J_3 C1/C2/C3),
- Upper Jurassic crystalline limestones, micritic limestones, and organogenic limestones (J_3 B2),
- Upper Jurassic marlstones, clayey-marly, and calcareous-marly sediments (J_3 B1+A),
- Middle Jurassic claystones, siltstones, and sandstones (J_2, sub-deposit layers).

Considering the geological structure of the deposit, lithostratigraphic units, and the depth range of each unit, 6 layers were distinguished in the numerical model: Quaternary clays, sands, and gravels (overburden – layers 1 and 2), Upper Jurassic limestones, marlstones, and marly limestones (layers 4, 5, and 6), and Middle Jurassic claystones, siltstones, and sandstones (layer 7). The mechanical parameters of each layer used in numerical modelling are presented in the table below (TABLE 3). The parameters of each layer were derived from those presented above (TABLE 1), but reduced by 10% (TABLE 3). Since displacements were not analysed and only stability was assessed, uniform elastic properties were adopted: Young's modulus E = 82 MPa and Poisson's ratio ν = 0.35. These parameters are generally considered to have a negligible influence on the factor of safety [30].

The 3D numerical model consisted, depending on the variant, of approximately 3.5 to 3.8 million cubic elements, with edge lengths ranging from 2 meters near the excavation surface, through 4 meters near the boundaries of defined layers, to 8 meters in other areas. The dimensions of this 3D numerical model are 1400 m × 600 m × 280 m. Numerical analysis was performed using the Modified Shear Strength Reduction (MSSR) method [31,32] with the application of FLAC3D software [33]. MSSR is a variant of the classical Shear Strength Reduction (SSR) method [34], differing in that it seeks the factor of safety (FS) by progressively reducing shear-strength parameters until the model becomes unstable, instead of narrowing the interval of values by bracketing, as in the classical SSR method. Once the first failure state is detected, the reduction is continued to track additional local instabilities, thereby revealing a set of plausible slip mechanisms with associated FS values. This approach is particularly useful for large, layered, or bench-cut slopes where assuming a single critical surface is an oversimplification. In this study, MSSR was applied to the Mohr-Coulomb material model.

The numerical analyses was divided into two stages:

- stability evaluation of the initial variant of northern slope geometry related to the deepening of pit wall slopes to the elevation of -20 m a.s.l. and identification areas with the lowest safety factor,
- redesigning the slope geometry and stability evaluation of the modified variant of the northern slope geometry.

The initial variant of the northern slope geometry is shown in Fig. 7, while the modified variant is presented in Fig. 8. The slope geometry was created based on the map provided by the mine, following appropriate processing. The surface mesh with a point spacing of 2 m × 2 m was generated through triangulation/linear interpolation procedures. Subsequently, surfaces for the individual geological layers were created using the Kriging method. The boundary between

the Upper and Middle Jurassic beds was based on limited geological data; thus, its course may differ from the actual position.

TABLE 3

Average geotechnical parameters for all layers included in the numerical model

No.	Strata/age	ρ [g/cm^3]	c [kPa]	φ [°]	Rr [kPa]
1	clays and silty clays (Q)	2.0	20	20.0	1
2	sands, gravels, and sandy clays (Q)	2.0	5	30.0	1
3	limestones, marly limestones, and marlstone C1/C2/C3 (J_3)+ B3/B4 (J_3)	2.60	154	26.05	77
4	crystalline limestones, micritic limestones, and organogenic limestones B2 (J_3)	2.72	364	38.78	182
5	marlstone, clayey-marly, and calcareous-marly sediments B1+A (J_3)	2.51	128	22.9	64
6	claystones, siltstones, and sandstones (J_2)	2.17	62	13.75	31

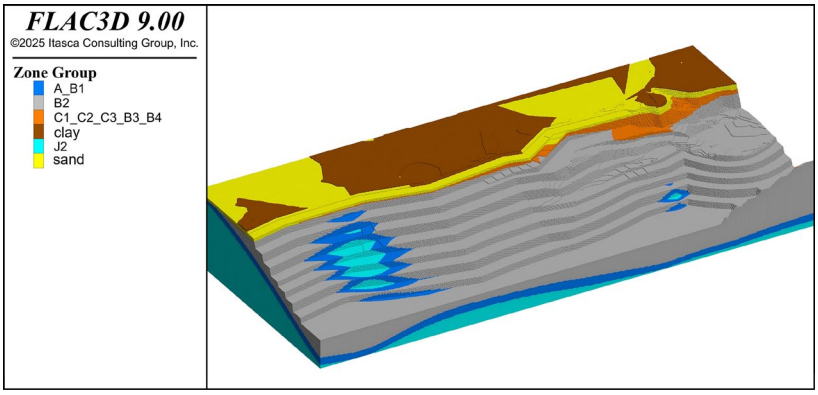

Fig. 7. The 3D model of the northern slope initial geometry

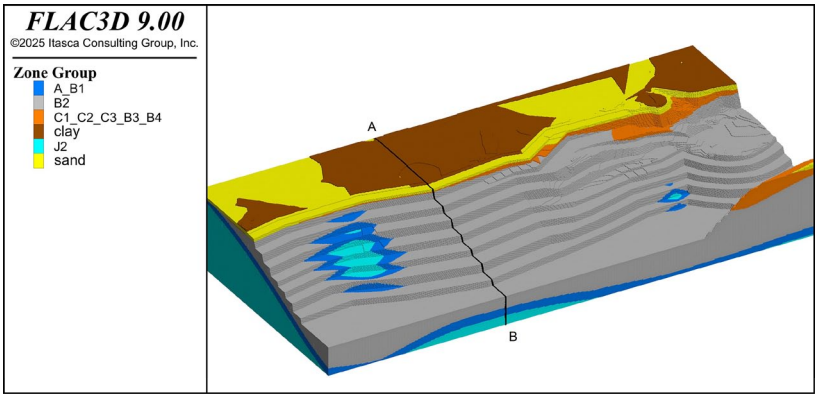

Fig. 8. The 3D model of the northern slope modified geometry

In addition to the 3D model, the 2D cross-sections were analyzed (Fig. 9), in which the mesh was densified by halving the element dimensions. The location of this 2D cross-section for the variant with the modified geometry is shown in Fig. 8 (A-B line).

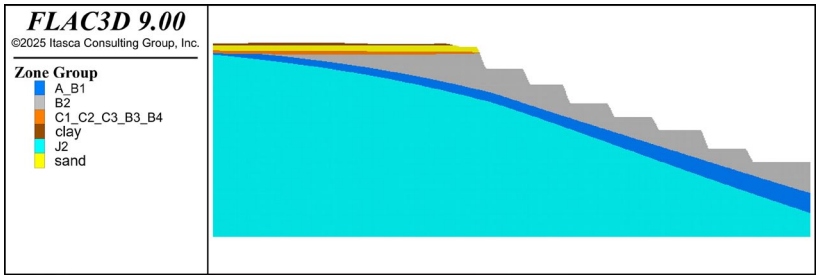

Fig. 9. 2D cross-section (A-B) – modified geometry variant of the northern slope

4. Results of numerical modeling

The result of the numerical analysis conducted for the northern slope of the Western Bielawy open-pit mine was prepared as a set of maps illustrating areas with specific values of the safety factor (SF), which can be interpreted using the accompanying legend (Fig. 10-12).

The classification of slope stability hazard according to the factor of safety (FS) was introduced by Nowacki et al. [35]:

- landslide occurrence is considered very unlikely for FS ≥ 1.5;
- landslide occurrence is considered unlikely for 1.3 ≤ FS < 1.5;
- landslide occurrence is regarded as probable for 1.0 ≤ FS < 1.3;
- landslide occurrence is regarded as highly probable for FS < 1.0.

In Polish open-pit mining practice, a threshold criterion of FS ≥ 1.3 is generally adopted for slope stability assessment.

The first stage of the numerical simulation indicated that deepening the pit wall slopes to the elevation of –20 m a.s.l. resulted in the SF ranging from 1.18 to 1.20 (Fig. 10). The areas with the lowest SF (1.00-1.10) were marked in Fig. 9 by a dark blue colour. These areas are related to the overburden sediments, such as sands and clays. The geometry of the overburden slope is shaped during preparatory work, in advance of the extraction front. The overburden slope and the excavation benches are shaped at this stage. Due to their thin thickness, these layers have minimal impact on the overall stability of the northern slope of the open-pit mine. In practice, overburden slopes are formed during the process of deposit access and generally exhibit gentler inclinations than those assumed in the analytical model. Due to the insufficient characterization of the overburden strata at the stage of the present study, the slope inclinations within these formations were not specified. Instead, the inclination of the overburden slopes was conservatively assumed to correspond to that of the upper bench of the limestone deposit slope, in order to provide a safe estimate of the loading conditions for slopes composed of soil and Quaternary strata like clays, sands, gravels, and sandy clays. In the western part of the northern slope, there are areas characterized by an SF ranging from 1.18 to 1.20, marked by green (Fig. 10). These areas are associated with local signs of karstification in the limestone beds (B2), such as cavi-

ties filled with calcite or clayey material, as well as the occurrence of marlstone, clayey-marly limestones, and calcareous marlstone (A1+B).

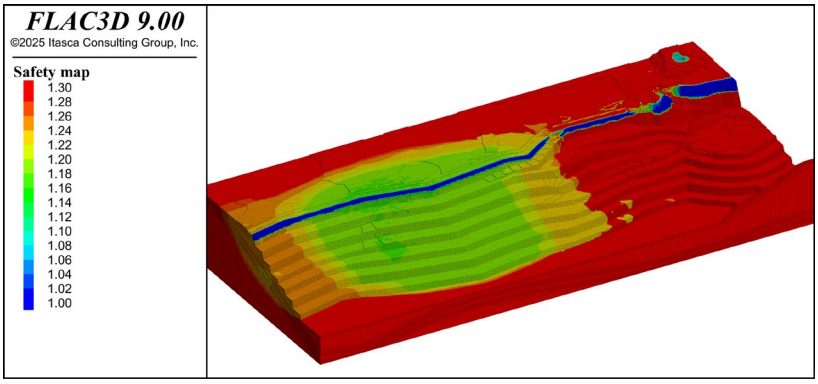

Fig. 10. Factor of safety contours of the initial geometry of the northern slope

To improve the stability conditions obtained in the first stage of numerical simulations, the slope geometry in problematic areas was modified by widening the +14 bench by 10 m and the –6 bench by 20 m. These changes resulted in a decrease in the slope angle from 22.48 degrees to 20.92 degrees (Fig. 11).

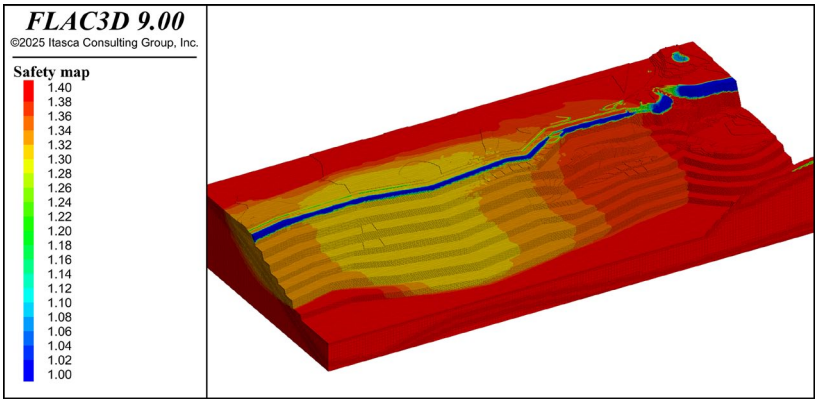

Fig. 11. Factor of safety contours of the modified geometry of the northern slope

The second stage of the 3D stability analysis was conducted for the modified slope geometry according to the changes described above. The implemented changes in the bench width and slope angle resulted in an increase in SF. The area in the western part of the slope reached an SF of 1.30-1.34, marked by orange colour (Fig. 11).

However, the 3D numerical simulation revealed that the deepened slope geometry locally intersects underlying (J_2) claystone beds. These claystones were severely fractured, fragmented

into cubes, and slickensided as a result of tectonic processes. Moreover, the drilling cores showed that at the boundary between J_2 and J_3 beds, limestones and marlstones were locally brecciated. Therefore, it is recommended to decrease the lower benches in these parts of the slopes where Middle Jurassic beds will be exposed during the excavation.

As mentioned in the previous section, the stability analysis of the modified geometry was also conducted in the 2D cross-section (Fig. 12). Despite the smaller mesh elements ensuring more detailed simulations, the 2D numerical analysis showed slightly higher FS (1.34-1.38) than the value obtained from the 3D analysis. These results contradict the generally accepted statement that the SF in 2D simulations is lower than in 3D analysis [36].

An analysis of the plasticity zones in the 2D cross-section (Fig. 13) reveals the presence of a potential slip surface predominantly developed within the Middle Jurassic beds. As mentioned before, these beds (claystones) were severely affected by shear deformation mechanisms. However, in the upper segment of this potential slip surface, which is situated within the B2 sediments, the failure was driven by extensional stresses leading to tensile fracturing.

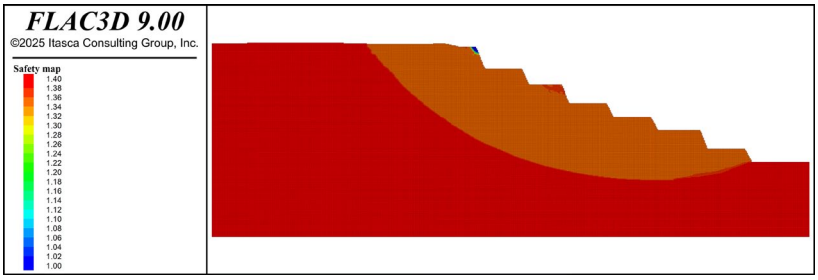

Fig. 12. Factor of safety contours of the 2D cross-section

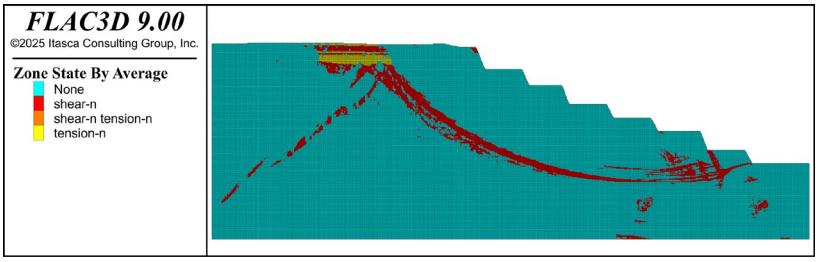

Fig. 13. Plasticity zones for 2D cross-section analysis

5. Conclusions

This study aimed to investigate the influence of complex geological conditions, including karst processes, tectonic disturbances, and lithological variability, on the stability of the northern slope in the Western Bielawy limestone open-pit mine, with the goal of optimizing excavation designs for safe and efficient deposit utilization. An integrated approach was adopted, combining laboratory testing of core samples to determine mechanical properties, detailed rock mass char-

acterization and 3D numerical modelling to simulate slope behaviour under planned geometries. The results of this integrated analysis revealed several key findings regarding the slope stability.

1. The planned deepening of the northern slope results in a decrease in the SF to 1.18, which is below the required value of 1.30. This low SF was caused by local signs of karstification in the limestones and the occurrence of marlstone, clayey-marly limestone and calcareous marlstone. Moreover, the local occurrence of brecciated limestones and marlstone at the boundary between Upper and Middle Jurassic beds, as well as tectonically disturbed Middle Jurassic claystones, contributed to the decrease in SF.
2. To ensure the stability of the northern slope, its geometry was modified by decreasing the overall slope angle from 22.48 degrees to 20.92 degrees by widening the +14 and -6 benches. The modified slope geometry resulted in an improvement of the SF to the required value of 1.30.
3. The presented analyses also showed that, due to the spatially variable geometry and geology, the two-dimensional cross-sectional analyses yielded a more optimistic SF (1.34) compared to the three-dimensional analyses (1.30). This difference confirms the necessity of conducting three-dimensional stability analyses for open-pit mines. In the case of slopes with irregular geometry and complex geology, where the stratigraphy and lithology vary significantly between adjacent cross-sections, three-dimensional analyses are recommended, as they are likely to provide more reliable values of the factor of safety and higher accuracy in slope stability assessment.
4. The results from the analysis demonstrate how detailed geotechnical description of the samples is essential for the reliable determination of mechanical parameters, as it provides a more accurate representation of the in-situ conditions. This has a significant influence on the outcomes of the numerical analysis results. Moreover, the performed analysis showed how tailored mining solutions can improve the stability of slopes under challenging geological conditions. The findings can be applied to similar mining operations located in carbonate formations affected by tectonic and weathering processes.
5. However, despite the advantages of 3D numerical modelling in capturing complex geological variability, the approach is limited by high computational demands, which extend simulation times and restrict the feasibility of even finer mesh resolutions or more extensive parametric studies; additionally, achieving higher accuracy requires further detailed geological reconnaissance, including additional boreholes and advanced geophysical surveys to better characterize karst features, tectonic disturbances, and lithological transitions.

In the future, with advancements in computational power, probabilistic analyses of the numerical modelling results could be conducted to account for uncertainties in geotechnical parameters and geological structures, providing a more robust assessment of slope stability risks that is currently infeasible due to the limitations of existing hardware.

Acknowledgements

The authors would like to express their sincere gratitude to Holcim Polska Kujawy Mining Plant for providing access to the geological and geotechnical data that made this research possible. Their support and willingness to share valuable information greatly contributed to the quality and comprehensiveness of this study.

References

[1] M. Rezaei, S.Z.S. Mousavi, Slope stability analysis of an open pit mine with considering the weathering agent: Field, laboratory and numerical studies. Engineering Geology **333**, 107503 (2024). DOI: https://doi.org/10.1016/j.enggeo.2024.107503

[2] F. Zhang, T. Yang, L. Li, L. Bu, T. Wang, P. Xiao, Assessment of the rock slope stability of Fushun West Open-pit Mine. Arabian Journal of Geosciences **14**, 1459 (2021). DOI: https://doi.org/10.1007/s12517-021-07815-8

[3] F. Zhang, T. Yang, L. Li, X. Zhu, Investigation on the reinforcement effect of a bedding slope affected by a landsliding block. Arabian Journal of Geosciences **15**, 528 (2022). DOI: https://doi.org/10.1007/s12517-022-09710-2

[4] A. Saadoun, A. Hafsaoui, Y. Khadri, M. Fredj, R. Boukarm, R. Nakache, Study Effect of Geological Parameters of the Slope Stability by Numerical Modelling, Case Limestone Career of Lafargem'sila, Algeria. IOP Conf. Series: Earth and Environmental Science **221**, 012021 (2019). DOI: https://doi.org/10.1088/1755-1315/221/1/012021

[5] T.-T. Yang, W.-H. Shi, P.-T. Wang, H.-L. Liu, Q.-L. Yu, Y. Li, Numerical simulation on slope stability analysis considering anisotropic properties of layered fractured rocks: a case study. Arabian Journal of Geosciences **8**, 5413-5421 (2015). DOI: https://doi.org/10.1007/s12517-014-1609-2

[6] M.A. Azizi, I. Marwanza, S.A. Amala, N.A. Hartanti, Three dimensional slope stability analysis of open pit limestone mine in Rembang District, Central Java. IOP Conference Series: Earth and Environmental Science **212**, 012035 (2018): DOI: https://doi.org/10.1088/1755-1315/212/1/012035

[7] B. Azarfar, S. Ahmadvand, J. Sattarvand, B. Abbasi, Stability Analysis of Rock Structure in Large Slopes and Open-Pit Mine: Numerical and Experimental Fault Modeling. Rock Mech. Rock. Eng. **52**, 4889-4905 (2019). DOI: https://doi.org/10.1007/s00603-019-01915-4

[8] G. Bezie, E.T. Chala, N.Z. Jilo, S. Birhanu, K.K. Berta, S.M. Assefa, B. Gissila. Rock slope stability analysis of a limestone quarry in a case study of a National Cement Factory in Eastern Ethiopia. Sci. Rep. **14**, 18541 (2024). DOI: https://doi.org/10.1038/s41598-024-69196-8

[9] C.A. Amagu, Ch. Zhang, J. Kodama, K. Shioya, T. Yamaguchi, A. Sainoki, D. Fukuda, Y. Fujii, M. Sharifzadeh, Displacement Measurements and Numerical Analysis of Long-Term Rock Slope Deformation at Higashi-Shikagoe Limestone Quarry, Japan. Advances in Civil Engineering, 1316402 (2021). DOI: https://doi.org/10.1155/2021/1316402

[10] W. Liu, G. Sheng, X. Kang, M. Yang, D. Li, S. Wu, Slope Stability Analysis of Open-Pit Mine Considering Weathering Effects. Appl. Sci. **14**, 8449 (2024). DOI: https://doi.org/10.3390/app14188449

[11] X. Li, Y. Jiang, S. Sugimoto, Slope stability analysis under heavy rainfall considering the heterogeneity of weathered layers. Landslides **22**, 1257-1273 (2025). DOI: https://doi.org/10.1007/s10346-024-02404-8

[12] J.A. Onyango, T. Sasaoka, H. Shimada, A. Hamanaka, D. Moses, Stability Assessment of the Slopes of an Oceanside Coral Limestone Quarry under Drawdown Condition of Semidiurnal Ocean Tides. Mining **2** (3), 589-615 (2022). DOI: https://doi.org/10.3390/mining2030032

[13] K. Liu, H. Li, Sh. Pang, M. Mi, J. Chen, K. Sun, Numerical Simulation Analysis of Slope Instability and Failure of Limestone Mine in Weibei. Advances in Civil Engineering, 5991348, (2021). DOI: https://doi.org/10.1155/2021/5991348

[14] H. Pomianowska, Warunki hydrogeologiczne w rejonie kamieniołomów Wapienno i Bielawy na Kujawach. Przegląd Geologiczny **44** (11), 1145-1151 (1996). https://geojournals.pgi.gov.pl/pg/article/view/18708/14724

[15] M. Dadlez, S. Marek, Utwory jurajskie struktury Zalesia na Kujawach i ich znaczenie surowcowe. Wydawnictwo Geologiczne, Warszawa 19-29 (1985).

[16] R. Dadlez, M. Narkiewicz, R.A. Stephenson, M.T.M. Visser, J.D. van Vees, Tectonic evolution of the Mid-Polish Trough, modelling implications and significance for central European geology. Tectonophysics **252**, 179-195 (1995). DOI: https://doi.org/10.1016/0040-1951(95)00104-2

[17] S. Rybicki, J. Legutko, Warunki geologiczno-inżynierskie złoża wapieni KCH „Kujawy" oraz wytyczne do projektowania geometrii zboczy wyrobisk i zwałowisk. Katedra Geologii Inżynierskiej i Geotechniki Środowiska, AGH (1996).

[18] R.J. Sokołowski, W. Wysota, Differentiation of subglacial conditions on soft and hard bed settings and implications for ice sheet dynamics: a case study from north-central Poland. Int. J. Earth Sci. **109**, 2699-2717 (2020). DOI: https://doi.org/10.1007/s00531-020-01920-x

[19] B. Matyja, T. Merta, A. Wierzbowski, Stratygrafia i litologia utworów jurajskich struktury Zalesia na Kujawach i ich znaczenie surowcowe. W: Dadlez M., Marek S., Utwory jurajskie struktury Zalesia na Kujawach i ich znaczenie surowcowe. Wydawnictwo Geologiczne, Warszawa 19-29 (1985).

[20] Digital geological map – Polish Geological Institute DOI: https://geologia.pgi.gov.pl/karto_geo/

[21] L. Machniak, Dodatek nr 4 do Projektu Zagospodarowania Złoża wapieni i margli jurajskich Barcin-Piechcin-Pakość wraz z kopaliną towarzyszącą w postaci piasków kwarcowych. Fundacja Nauka i Tradycje Górnicze AGH, (2018).

[22] E. Hoek, E.T. Brown, Underground excavations in rock. London. Instn Min. Metall. (1980). DOI: https://doi.org/10.1201/9781482288926

[23] E. Hoek, E.T. Brown, Empirical strength criterion for rock masses. J. Geotech. Engng Div., ASCE 106 (GT9), 1013-1035 (1980). DOI: https://doi.org/10.1061/AJGEB6.0001029

[24] E. Hoek, P. Marinos, Predicting tunnel squeezing problems in weak heterogeneous rock masses. Tunnels and Tunnelling International **132** (11), 45-51 (2000).

[25] P. Marinos, V. Marinos, E. Hoek, Geological Strength Index (GSI). A characterization tool for assessing engineering properties for rock masses. Published in: Underground works under special conditions, eds. Romana, Perucho & Olalla, 13-21, Lisbon: Taylor and Francis (2007).

[26] D.U. Deere, D.W. Miller, The Rock Quality Designation (RQD) Index in Practice, Classification Systems for Engineering Purposes. ASTM STP, American Society for Testing and Materials, Philadelphia, PA, 91-101 (1967). DOI: https://doi.org/10.1520/STP48465S

[27] E. Hoek, T.G. Carter, M.S. Diederichs, Quantification of the Geological Strength Index chart. 47th US Rock Mechanics /Geomechanics Symposium **3**, 1757-1764 (2013).

[28] T. Bieniawski, 1989. Engineering rock mass classifications: a complete manual. John Wiley & Sons, New York.

[29] H. Pomianowska, Dokumentacja z wykonania otworów obserwacyjnych na terenie Zakładu Górniczego Kujawy w Bielawach LAFARGE CEMENT S.A. Geofizyka Toruń, Materiały Archiwalne ZG Kujawy (2018).

[30] J.R. Stianson, D. Chan, D.G. Fredlund, Comparing slope stability analysis based on linear elastic or elasto plastic stresses using dynamic programming techniques. 57th Canadian Geotechnical Conference, 5th Joint CGS/IAH-CNC Conference (2004), Session 7C (23-30).

[31] M. Cała, J. Flisiak, Analiza stateczności skarp i zboczy z zastosowaniem zmodyfikowanej metody redukcji wytrzymałości na ścinanie, Geotechnika w budownictwie i górnictwie. Oficyna Wydawnicza Politechniki Wrocławskiej, Wrocław, 348-354 (2003).

[32] M. Cała, J. Flisiak, A. Tajduś, Slope stability analysis with FLAC in 2D and 3D, 4th International FLAC Symposium on Numerical Methods in Geomechanics (edited by Hart & Varona), 11-14 (2006).

[33] FLAC3D 9.0 Manual, Itasca Software (2024).

[34] O.C. Zienkiewicz, C. Humpheson, R.W. Lewis, Associated and non-associated visco-plasticity and plasticity in soil mechanics. Geotechnique **1**, 25 (4), 671-689 (1975). DOI: https://doi.org/10.1680/geot.1975.25.4.671

[35] J. Nowacki, J. Naborczyk, J. Petrasz, A. Sala, Instrukcja obserwacji i badań osuwisk drogowych, Generalna Dyrekcja Dróg Publicznych, Wydawnictwo Print Kraków (1999).

[36] M. Xie, Z. Wang, X. Liu, B. Xu, Three-dimensional critical slip surface locating and slope stability assessment for lava lobe of Unzen volcano. Journal of Rock Mechanics and Geotechnical Engineering **3** (1), 82-89 (2011). DOI: https://doi.org/10.3724/SP.J.1235.2011.00082